Methodology for Flow and Salinity Estimates in the Sacramento-San Joaquin Delta and Suisun Marsh

23rd Annual Progress Report
June 2002

Chapter 2: Particle Tracking Model Verification and Calibration

Author: Aaron Miller

2 Particle Tracking Model Verification and Calibration

2.1 Introduction

The Particle Tracking Model (PTM) is one of three modules of the California Department of Water Resource's Delta Simulation Model 2 (DSM2). DSM2 is a combination of three models: HYDRO, a hydrodynamics model; QUAL, a water quality model; and a particle tracking model PTM. PTM simulates the movement of neutrally buoyant particles using transport principles when given hydrodynamic information from HYDRO.

PTM was last validated early in the year 2000 (Wilbur, 2000). Since this time, two things occurred which warranted another model calibration and validation. First, the hydrodynamic model was recently recalibrated, which resulted in changed flow patterns and updated channel bathymetry (Nader-Tehrani, 2001). The method used to represent open water areas was also changed. Second, the formulation of the mixing equations was modified. The formulation for particle mixing was altered to include point velocities at the location of the particle. Also in this formulation is the inclusion of a particle drift term. This drift term is required to keep the mixing equations consistent with the transport equations.

This chapter describes the process and results for the verification and calibration of the PTM. The formulation of PTM was verified by comparing it with theoretical dispersion. The velocity profiles the model uses to generate quasi 3-dimensional velocity fields were calibrated using field-measured velocity. Validation of the model was completed using the 1997 dye study (Oltmann, 1998).

2.2 Background

The Delta Modeling Section began development of the Particle Tracking Model in 1993. Smith (1993) developed the first model in FORTRAN for DSM1 using a formulation developed by Gib Bogle (Water Engineering and Modeling, 1994). The original model was a quasi 2-dimensional model. It was further modified to a quasi 3-dimensional model. Nicky Sandhu and Ralph Finch (DWR) converted the model to Java in 1997.

Since the first Java version of the model there have been advancements in simulating particle behavior, the incorporation of water quality, and implementation of an enhancement to the mixing formulation. Gib Bogle also developed the enhancement to the mixing with assistance from Richard Denton (Contra Costa Water District). Miller (2000) added this enhancement to the code and has further developed particle behavior sections of the code.

2.3 PTM Theory

The dispersion coefficient, *K*, is defined as one half the change in variance with respect to time. This is shown in Figure 2.1.

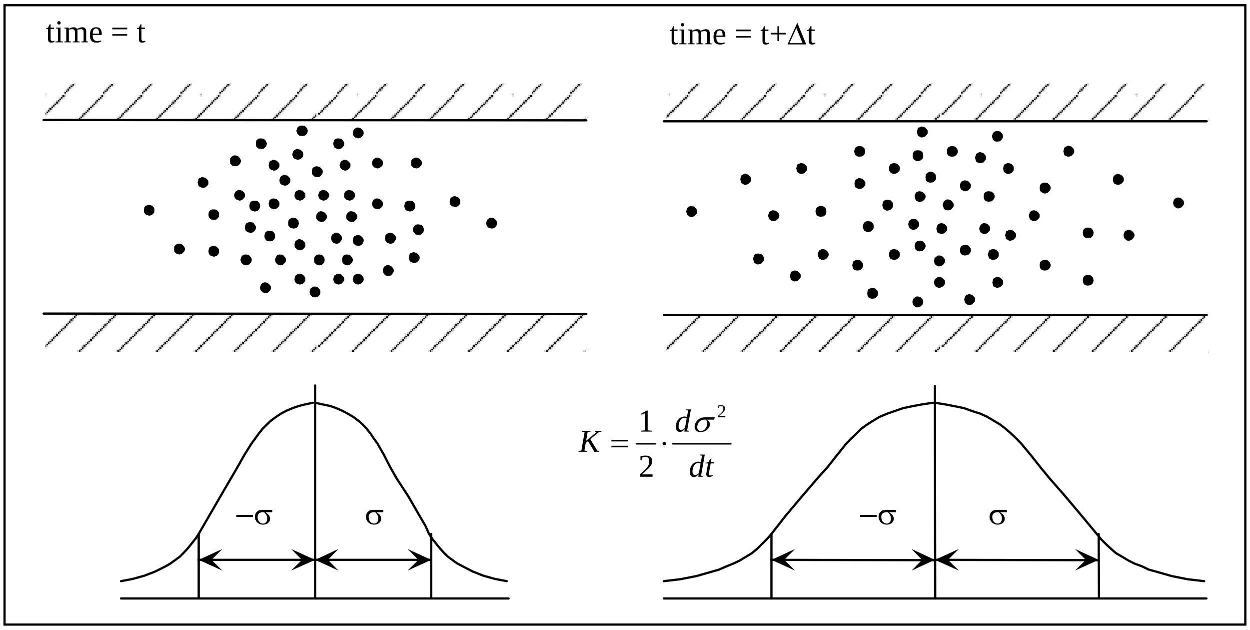

Figure 2.1: Definition of Dispersion Coefficient, *K*.

Equation 2-1 defines the derived dispersion coefficient, *K*.

$$K = \frac{h^2 \overline{u}'^2 I}{\overline{\varepsilon}_t} \qquad \text{[Eqn. 2-1]}$$

where,

K	=	dispersion coefficient,
h	=	characteristic length,
$\overline{u}'$	=	expected squared of the deviation of the depth-averaged velocity,
I	=	dimensionless integral of the velocity profile, and
$\overline{\varepsilon}_t$	=	transverse mixing coefficient.

Fischer et al. (1979) report characteristic lengths that range from half to the full width of the channel cross-section. The integral of the velocity profile is nearly constant for real streams, and ranges from 0.01 to 0.03 (Bogle, 1997). The expected squared of the deviation of the depth-averaged velocity is based on the difference from the actual velocity, u, by the mean velocity, $\overline{u}$, and is described by Fischer et al. (1979) as ranging from $0.03\overline{u}^2$ to $0.20\overline{u}^2$.

2.3.1 Longitudinal Dispersion

To model dispersion, PTM utilizes flow and cross-sectional area provided by HYDRO. This flow is one-dimensional and, when used to calculate velocity, assumes a uniform velocity across a channel cross-section. Using a one-dimensional model for flow and stage calculations is relatively efficient and accurate for the majority of the Delta. However, PTM utilizes the calculated velocity to determine particle movement. PTM depends on differential velocities to simulate dispersion, but a one-dimensional model does not provide a differential velocity field. Thus, theoretical profiles were applied to HYDRO's one-dimensional velocities. The application of these profiles creates a quasi three-dimensional velocity field in the cross section. This velocity field forces particles to move at a speed determined by the combination of the vertical and the transverse profiles. This differential movement in the longitudinal direction creates a dispersive effect.

Equation 2-2 describes the point velocity in the longitudinal direction. Figure 2.2 shows the coordinate convention for a channel.

$$u(y,z) = \bar{u} \cdot F_T(y) \cdot F_V(z) \qquad \text{[Eqn. 2-2]}$$

where,

$\bar{u}$ = mean velocity,
$F_T(y)$ = transverse multiplication factor, and
$F_V(z)$ = vertical multiplication factor.

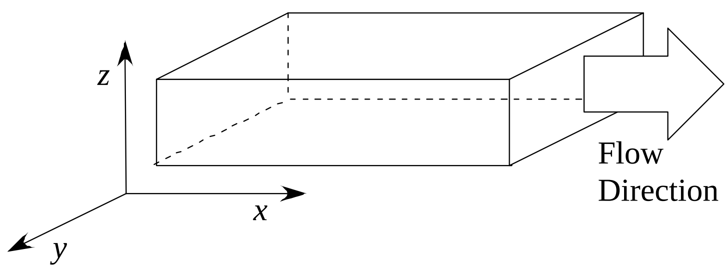

Figure 2.2: Coordinate Convention for a Channel.

When F_V and F_T are equal to one, the particle is traveling at the average velocity of the water in the channel. The functions F_V and F_T represent the profiles used to simulate dispersion. They are described in more detail below.

Vertical Profile

In the vertical direction the velocity profile is described by a von Karman logarithmic function. The von Karman logarithmic profile has been found to be a good approximation of vertical velocity profile in wide two-dimensional channels (Bogle, 1997). Wilbur (2000) added the shape factor to change the profile shape while conserving the von Karman constant.

$$F_V(z) = 1 + \frac{u^*/\overline{u}}{s \cdot k}\left[1 + \ln\left(\frac{z}{d}\right)\right] \qquad \text{[Eqn. 2-3]}$$

where,

u^* = shear velocity,
s = shape factor,
k = von Karman constant (≈0.4),
z = vertical position from the bottom of the channel, and
d = depth of channel from water surface.

The shear velocity used in Equation 2-3 is calculated as the shear velocity for steady flow in an open channel, as shown by Equation 2-4.

$$u^* = \sqrt{g \cdot r_h \cdot S} \qquad \text{[Eqn. 2-4]}$$

where,

g = acceleration due to gravity,
r_h = hydraulic radius, and
S = channel bottom slope.

Figure 2.3 shows examples of vertical profiles using different shape factors. As the shape coefficient, *s*, approaches zero the intercept of the profile moves to 0.37 of the depth and the maximum value of the profile moves towards infinity.

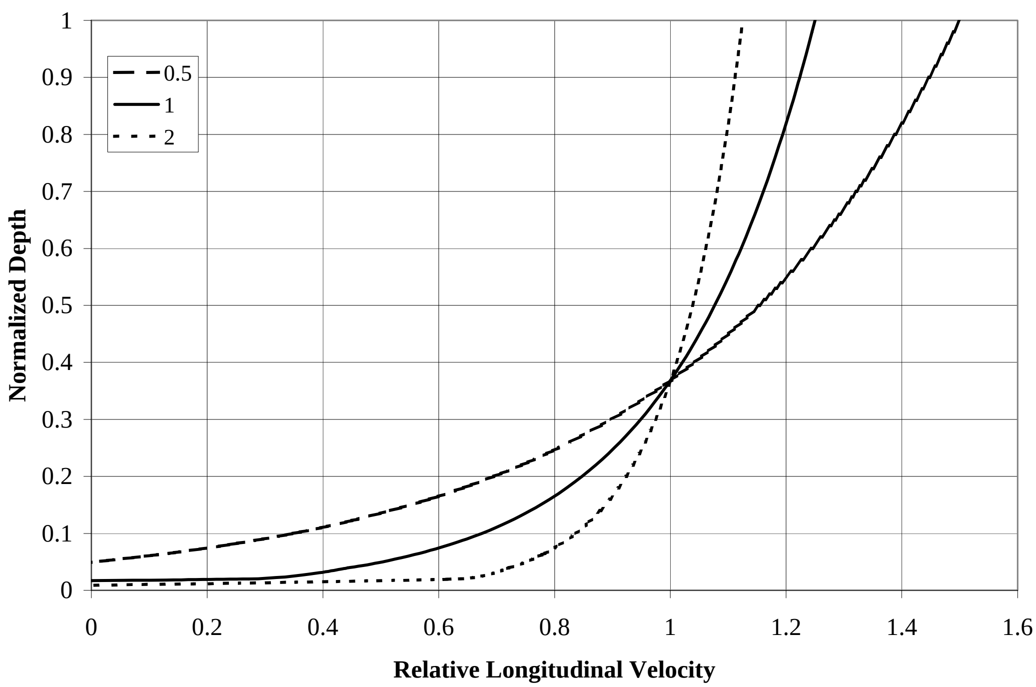

Figure 2.3: Examples of Vertical Profiles using Different Shape Factors, *s*.

Transverse Profile

In the transverse direction the velocity profile is described by a quartic function (Equation 2-5). Bogle (1997) arrived at this function through numerical experiments.

$$F_T(y) = A + B\left(\frac{2y}{w}\right)^2 + C\left(\frac{2y}{w}\right)^4 \qquad \text{[Eqn. 2-5]}$$

where,

A,B,C = profile shade coefficients,
w = channel width, and
y = transverse position from center of the channel.

Given that the velocity at the sides of the channel is equal to zero, Bogle (1997) simplified Equation 2-5 at the middle of the channel ($y = w/2$) to:

$$A + B + C = 0 \qquad \text{[Eqn. 2-6]}$$

To maintain the average velocity, the area of the profile is required to be a value of 1. Integrating Equation 2-5 where y is between $-w/2$ and $w/2$ and by dividing by the width, w, results in:

$$A + \frac{B}{3} + \frac{C}{5} = 1 \qquad \text{[Eqn. 2-7]}$$

When A is used at the free parameter, the maximum velocity occurs along the centerline at $y = 0$. Thus Equations 2-6 and 2-7 can be solved in terms of the remaining coefficients B and C:

$$B = -6A + 7.5 \qquad \text{[Eqn. 2-8]}$$

$$C = 5A - 7.5 \qquad \text{[Eqn. 2-9]}$$

For application in the Sacramento-San Joaquin Delta, A=1.2, B=0.3, and C=-1.5 was found to be representative of the velocity profiles found in the Delta channels (Wilbur, 2000).

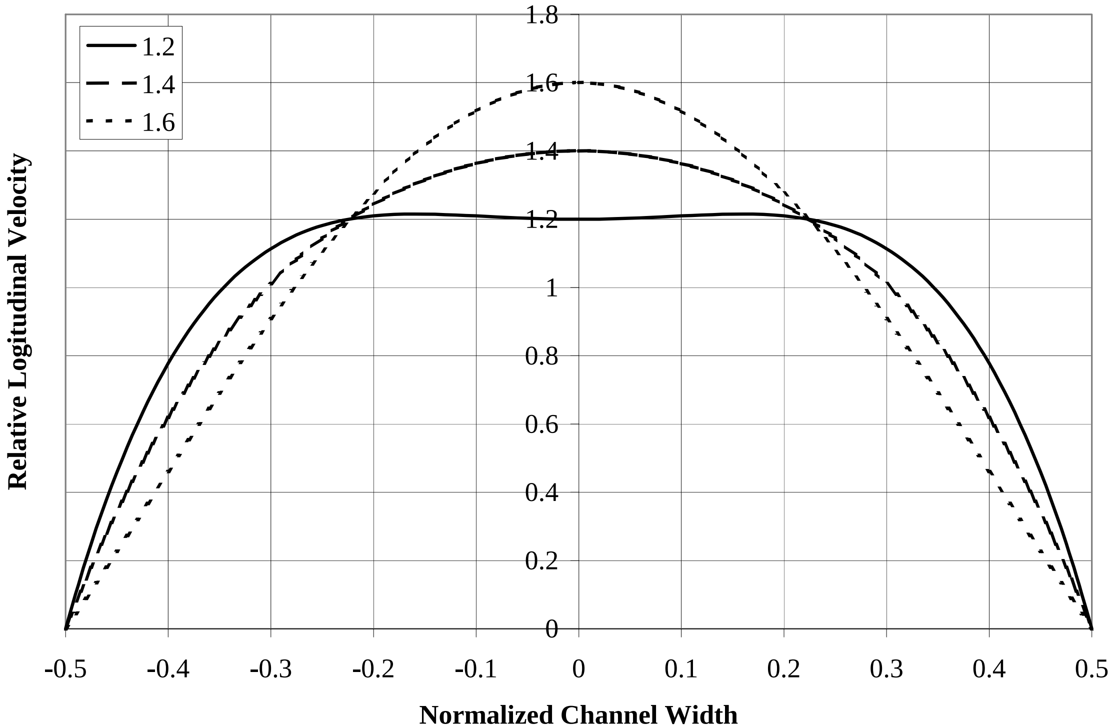

Figure 2.4: Example of Transverse Profiles with Coefficient, *A*, Ranging from 1.2 to 1.6.

Combining Vertical and Transverse Velocity Profiles

The point velocity is a function of the vertical and horizontal position in the channel. A particle at the top center of a channel will have a higher velocity than a particle near the side or bottom. For example, a position near the top center of the channel will have a point velocity around 1.5 times the average velocity for a vertical shape factor of 1 and a transverse shape coefficient *A* of 1.2, using Equation 2-2 and Figures 2.3 and 2.4. A position near the bottom or side of the channel will result in a point velocity approaching zero.

2.3.2 Longitudinal Diffusion

Particle movement within the channel cross section is completed through diffusion. Given a longitudinal velocity a particle will tend to move vertically and horizontally due to turbulent mixing. Because a one-dimensional hydrodynamics model is used for flow and velocity, the movement in the *y* and *z* direction must estimated using empirical equations.

Vertical Mixing

Vertical particle position in a channel is based on the normalized depth of the channel where 0 is the bottom of the channel and 1 is top of the water column (Figure 2.5). Movement in the vertical direction is estimated using a vertical diffusivity coefficient, ε_V, which is defined as one half the derivative of the variance of the vertical distance, σ_z^2, traveled in one time step (Equation 2-10). The empirical form of the vertical diffusivity coefficient, Equation 2-11, is based on the depth, average velocity, and vertical position in the channel. Fischer (1979) completed the initial derivation, and Wilbur (2000) added the shape factor to change the profile shape and to conserve the von Karman constant.

$$\varepsilon_V = \frac{d\sigma_z^2}{2dt} \qquad \text{[Eqn. 2-10]}$$

$$\varepsilon_V = sku^* z\left(1 - \frac{z}{d}\right) \qquad \text{[Eqn. 2-11]}$$

where,

s = shape factor,
k = von Karman constant,
u^* = shear velocity (see Equation 2-4),
z = vertical position from the bottom of the channel, and
d = depth of the channel from the water surface.

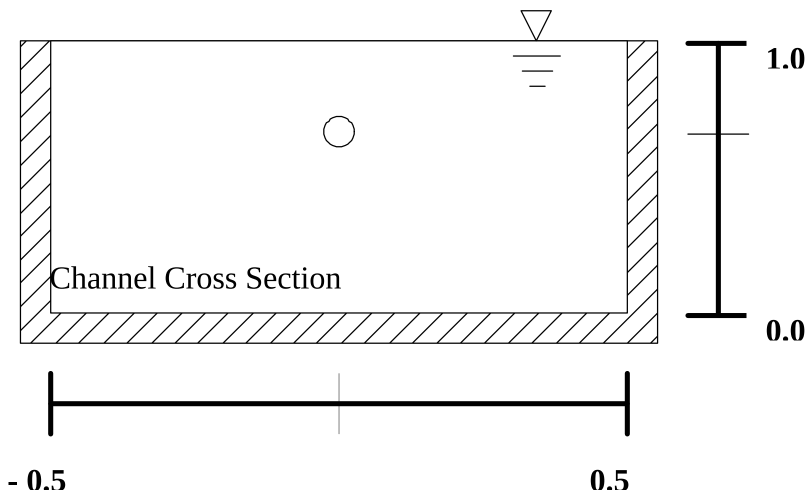

Figure 2.5: Diagram of Particle Position Coordinate Convention.

Smith (1998) showed the derivation of a particle's change in vertical position (Equation 2-10). The particle's change in vertical position, Δz, is then calculated using a Gaussian random number, the diffusivity coefficient, and the time step as described by Equation 2-12.

$$\Delta z = R\sqrt{2\varepsilon_V \Delta t} \qquad \text{[Eqn. 2-12]}$$

where,

R = Gaussian random number, with a mean of 0 and variance of 1, and
Δt = time step.

The current particle position, as given by Equation 2-13, is adjusted using the change in position and the gradient of the diffusivity for the time step. Denton (1995) showed that this gradient contribution was important in reducing particle drift for non-uniform mixing. Particle drift is the phenomena where particles move to certain locations in a channel and stay there. Dimou and Adams (1993) applied a similar gradient contribution or correction factor to a one-dimensional particle tracking model. In addition, this gradient contribution is required to obtain equivalence between the random walk algorithm (Fokker-Planck Equation) and the transport equation.

$$z_1 = z_0 + \Delta z + \frac{d\varepsilon_V}{dz}\Delta t \qquad \text{[Eqn. 2-13]}$$

The gradient of the vertical diffusivity coefficient is defined by Equation 2-14.

$$\frac{d\varepsilon_V}{dz} = sku^*\left(1 - 2\frac{z}{d}\right) \qquad \text{[Eqn. 2-14]}$$

Transverse Mixing

The transverse mixing is similar to the vertical mixing. The position of the particle in the transverse direction is based on the normalized width of the channel where –0.5 is the left bank, 0.5 is the right bank, and 0.0 is the center (Figure 2.5). Transverse movement is estimated using a transverse diffusivity coefficient, ε_T, which, like the vertical diffusivity, is defined as one half the derivative of the variance of the distance traveled in one time step, Equation 2-15. The empirical form of the transverse diffusivity coefficient, Equation 2-16, is based on a flow coefficient, average velocity, channel depth, and transverse velocity profile from Equation 2-5.

$$\varepsilon_T = \frac{d\sigma_y^2}{2dt} \qquad \text{[Eqn. 2-15]}$$

$$\varepsilon_T = C_T u^* d\left[A + B\left(\frac{2y}{w}\right)^2 + C\left(\frac{2y}{w}\right)^4\right] \qquad \text{[Eqn. 2-16]}$$

where,

C_T = flow coefficient,
A,B,C = profile shape coefficient,
y = transverse position from the center of the channel, and
w = channel width.

Smith (1998) showed the derivation of a particle's change in transverse position from Equation 2-15. The particle change in transverse position is then calculated using a Gaussian random number, the transverse diffusivity coefficient, and the time step as shown in Equation 2-17.

$$\Delta y = R\sqrt{2\varepsilon_T \Delta t} \qquad \text{[Eqn. 2-17]}$$

Like the vertical displacement, the current particle position, as given in Equation 2-18, is adjusted using the change in position and the gradient of the diffusivity for the time step. Denton (1995) showed why this gradient contribution was important. Dimou and Adams (1993) applied a similar gradient contribution or correction factor to a one-dimensional particle tracking model.

$$y_1 = y_0 + \Delta y + \frac{d\varepsilon_T}{dy}\Delta t \qquad \text{[Eqn. 2-18]}$$

The gradient of the transverse diffusivity coefficient was found to be defined by Equation 2-19.

$$\frac{d\varepsilon_T}{dy} = C_T u^* d\,\frac{2y}{w^2}\left[4B + 8C\left(\frac{2y}{w}\right)^2\right] \qquad \text{[Eqn. 2-19]}$$

2.3.3 Channel Boundaries

Currently PTM is not able to incorporate irregular cross-sections as HYDRO does. Irregular cross-sections are cross-sections that are not rectangular. PTM obtains cross-sectional information from HYDRO, and then builds a representative rectangular cross-section. As illustrated in Figure 2.6, PTM assumes the same depth as an irregular cross-section in HYDRO and then calculates the width for the given cross-sectional area.

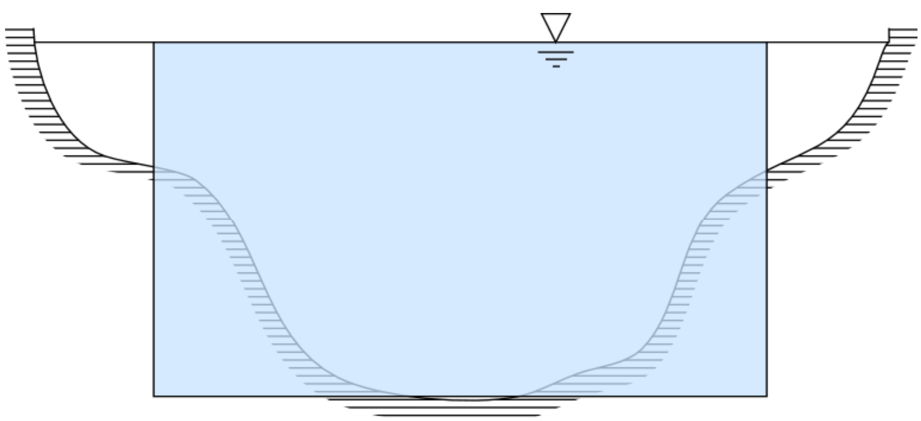

Figure 2.6: PTM Representation of an Irregular Channel where Width is Calculated for a Given Flow Area and Depth.

The PTM simulates the movement of particles within this rectangular cross-section. While calculating the particle movement, there are times when the calculated distance a particle should travel would result in the particle moving outside the boundary of this rectangle. In cases like this the particles “bounce” back into the channel the same projected distance as shown in Figure 2.7.

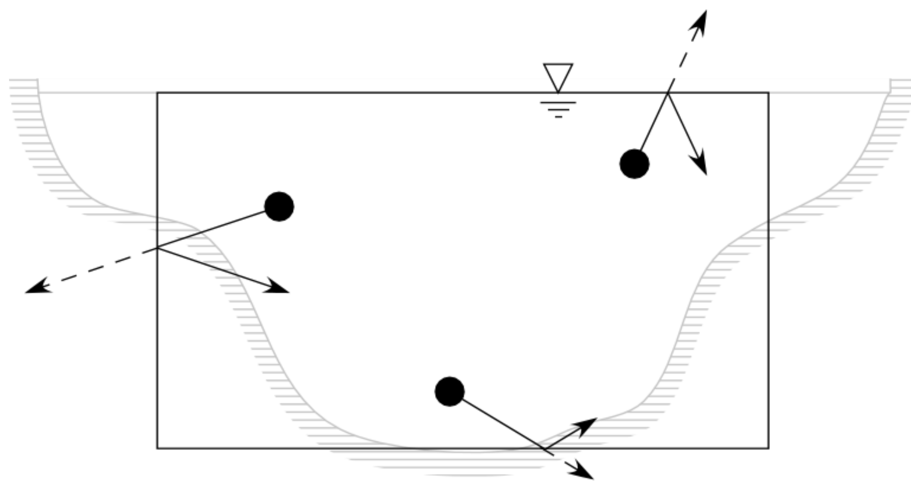

Figure 2.7: Particles Bounce the Same Projected Distance into the Channel.

Excessive bouncing occurs when particle movement is simulated with long time steps. With long time steps a particle movement may be calculated so that it is required to bounce off of the channel boundaries many times. Use of sub-time steps eliminates excessive bouncing. Sub-time steps are calculated by utilizing the channel depth or width, the velocity, and the mixing coefficient. The model currently does not allow the particle to move (and therefore bounce) more than 10% of the width or depth within one sub-time step.

2.3.4 Movement at Junctions

Decisions are made at various points within the simulation. At a junction the particle must decide which path to take. The path may lead to another channel, open water area, agricultural diversion, or an export. As illustrated in Figure 2.8, the path of a particle is determined randomly based on the proportion of flow. The proportion of flow determines the probability of movement into each reach (Equation 2-20). A random number based on this determined probability then determines where the particle will go.

$$P\left(particle\, entering\ water\, body\right) = \frac{flow\, entering\ water\, body}{total\ \ flow @\ junction} \qquad \text{[Eqn. 2-20]}$$

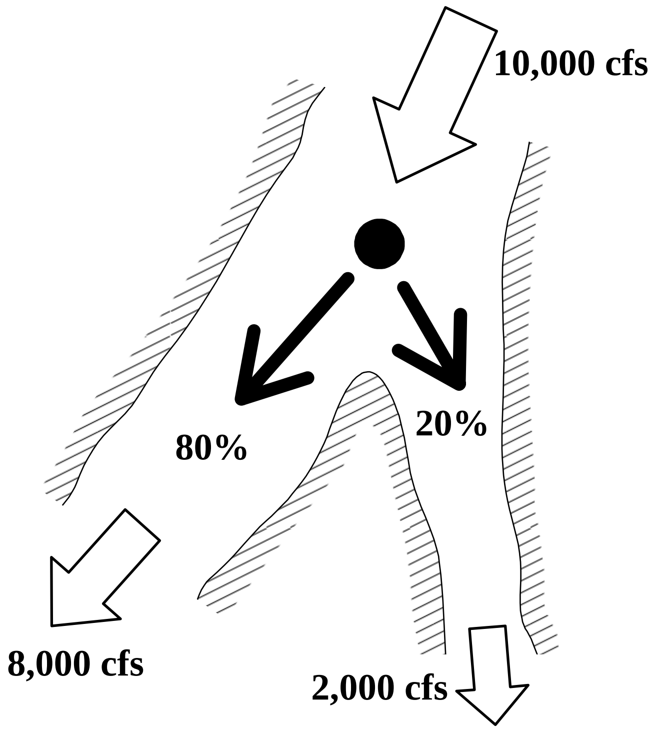

Figure 2.8: Probability Based Determination of a Particle Path at a Junction Flow Split.

2.3.5 Movement in and out of Open Water Areas

A particle that moves into an open water area, such as a reservoir, no longer retains its position information. A DSM2 open water area is considered a fully mixed reactor. The path out of the open water area is a decision based on the volume in the open water area, the time step, and the flow out of the area as shown in Equation 2-21.

$$P\left(particle\,entering\ water\ body \right) = \frac{flow\,entering\ water\ body \times time\ step}{open\,water\ area\,total\ volume} \qquad \text{[Eqn. 2-21]}$$

2.4 Profile Calibration

2.4.1 Estimation of Profile Coefficients

Profile coefficients were determined for both the transverse and vertical profiles using Acoustic Doppler Current Profiler (ADCP) transect data. The profile equations were simplified using the transect information. The transect information included average velocity, width, depth, and position in the channel. To simplify these equations into univariate relationships the coefficients were estimated using linear regression.

Transverse and vertical profile coefficients were determined by linear regression between simplified profile equations and measured field velocities. The measured velocities were obtained from United States Geological Survey (USGS) ADCP transects. These transects represent the three-dimensional velocity across a channel cross section at a time in history. Figure 2.9 shows the locations of the transect data used in this analysis. This process is explained in greater detail in the following paragraphs.

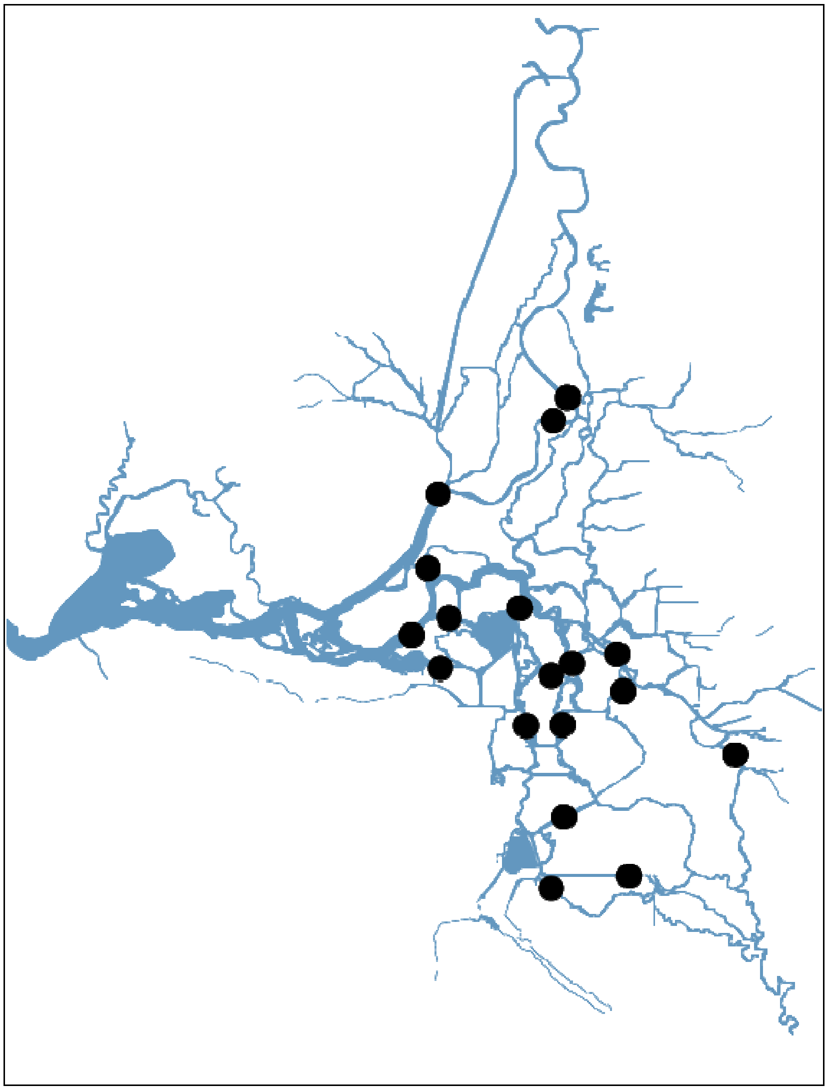

Figure 2.9: Location of Available ADCP Transects.

Field Measured Velocity

The field measurements used in estimating the velocity profile coefficients were provided by the USGS in the form of velocity transects. As shown in Figure 2.10, a transect is typically obtained by a boat-mounted ADCP that moves across a channel while taking several vertical velocity profile measurements (RD Instruments, 1995). The ADCP makes several velocity or *depth cell* measurements and then averages these into *ensembles*. Each *ensemble* then represents the average velocity for a 25 to 50 cm distance. The combination of *ensembles* then makes up a vertical velocity profile at the current ADCP position. The distance between the vertical velocity profiles is dependant on the speed of the boat and the time between samples.

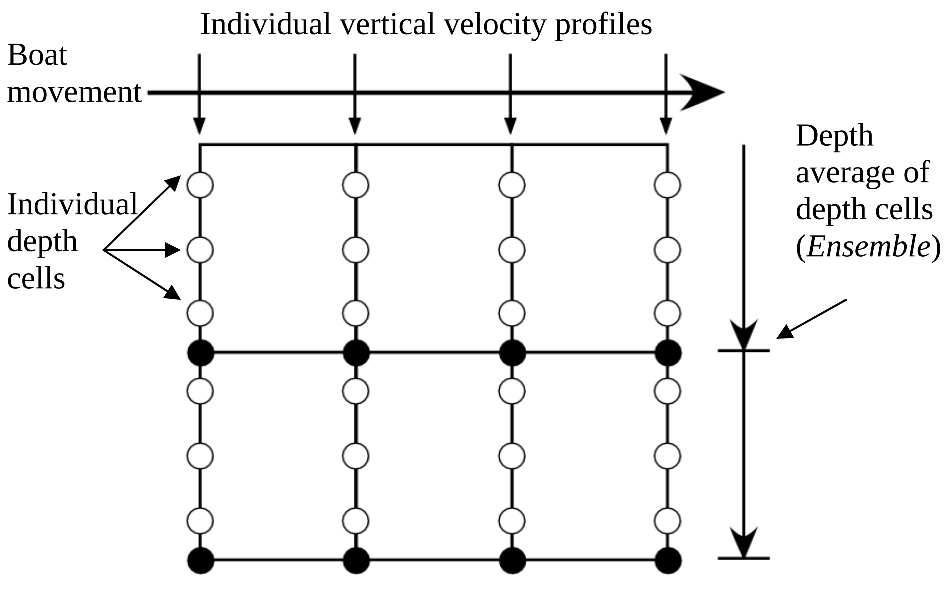

Figure 2.10: Creation of Depth Ensembles.

Data Manipulation

The data was adjusted for two main factors: 1) the distance between measured velocity profiles, and 2) the direction of the velocity vector. When the boat carrying the ADCP crosses a channel, the boat captain attempts to make the boat path as straight and perpendicular to the channel bank as possible. However, this is a difficult task especially in higher flows and the path tends to be less than perfect. As shown in Figure 2.11 the boat track can be straightened. In this process the starting and ending points of the boat track are preserved and the vertical velocity profiles are adjusted to the new reference line.

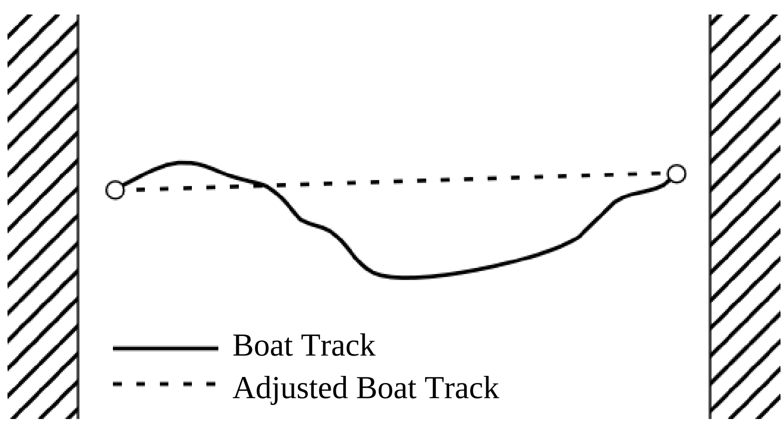

Figure 2.11: ADCP Boat Track and Adjusted Track.

The ADCP reports the velocities in a vertical profile as a series of three-dimensional vectors. To relate these data to PTM, these three-dimensional data were converted to one-dimension. A resultant vector was calculated for each transect to find the average direction of flow. This direction was then used to adjust the velocity vector direction and magnitude in the flow field. The adjusted boat track and the adjusted velocity direction are not necessarily perpendicular.

The transects provide a good coverage of velocity across a given channel. However, the transects lack the ability to capture detail at the top, the bottom, or the sides of a channel. The top of the cross-section is not included because the ADCP is submerged below the surface of the water. Typically the top one meter of the cross-section is lost, but this loss is not necessarily bad. The topmost portion of the water column can be heavily influenced by environmental conditions, such as wind. The velocities at the bottom of the transect are not recorded. The distance not recorded varies by cross section. This loss of velocity information at the bottom is essential for keeping track of the ADCP position with respect to the bottom of the channel. The velocity at the sides of the channel is also lost due to the inability of boat to safely reach the bank. The operators of the boat estimate the distance from the start and end of the boat track to the bank. Figure 2.12 illustrates the availability of data within a given cross-section. The gray squares represent the location and averaging that occurs when an ADCP is collecting data and creating the *ensembles*.

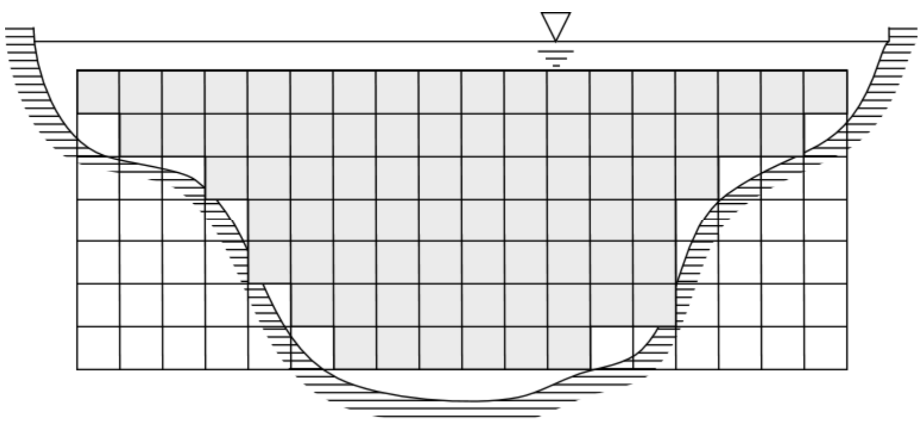

Figure 2.12: Velocity Coverage for a Channel Cross-Section (shown in gray).

For estimating the transverse profile coefficients the depth-averaged velocity was used. Similarly the vertical profile coefficients used the width-averaged velocity.

As illustrated in Figure 2.13, the width and the depth of the channel were estimated. The width of the channel includes both the straight-line distance of the transect and estimates from the transect start and end points to the channel banks. This total length was used in estimating the transverse profile coefficient. The depth of the channel was estimated using the ADCP. The estimated distance from the last velocity value in the profile to the bottom of the channel was calculated using ADCP estimated bottom error.

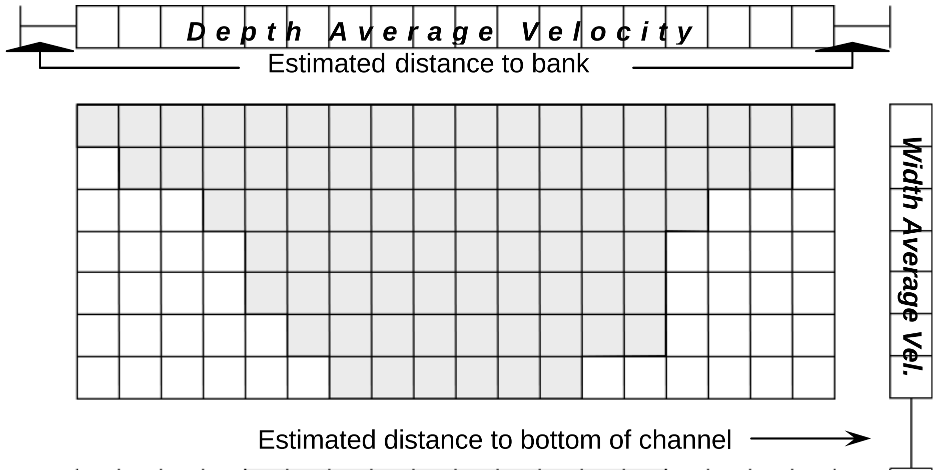

Figure 2.13: Transverse and Vertical Profiles Represent the Depth Averaged and Width Averaged Transect Values.

Filtering Data

The data for each cross section was examined and filtered before being added to the regression. Only data from cross sections with an average velocity greater than 0.25 ft/s were used. The solution for the coefficient of both the vertical and transverse profiles becomes unstable as the average velocity approaches zero. Also, profiles with lower velocities are typically in a flow transition, such as moving from flood to ebb tide. This flow transition is important in the dispersion process, but the velocities in these types of transects are very complex and difficult to model. Transects with average velocities greater than 0.25 ft/s typically have, or are in the process of forming, a velocity profile, which can be estimated more easily.

Additional limitations were placed on the data for the vertical profile. For each transect the shape coefficient was determined and data were used only if the coefficient was found to be greater than 0.5. This limitation was implemented to reduce the amount of outliers and eliminate unreasonable data. As the shape coefficient moves towards zero, the intercept of the profile moves to around 0.37 of the depth and the maximum value of the profile goes toward infinity (Figure 2.3).

For the transverse profile, like the vertical profile, a limitation was placed on the coefficient. For each transect the coefficient was determined and the data were not used if the coefficient was less than 1.25 or greater than 1.87. Values less than 1.25 describe profiles that are concave in the center. Values greater than 1.87 describe profiles that become negative near the sides.

Estimating Vertical Profile Coefficients

To estimate the vertical velocity coefficient, Equations 2-2 and 2-3 were combined. Combining these equations and assuming a width averaged velocity ($F_T(y) = 1$), the point velocity is then described by Equation 2-22. For each cross-section the width averaged velocity is used in the estimation of a vertical velocity profile. The point velocity (u) was the width averaged velocity at each layer. The average velocity ($\bar{u}$) was the average velocity of the average vertical velocity profile. The vertical position (z) was the height of the velocity layer above the bottom of the channel. The depth (d) was estimated using ADCP data. The unknown, von Karman constant, can be estimated using a $y=Ax$ model linear regression.

$$u - \bar{u} = \frac{1}{sk} u^* \left[1 + \ln\left(\frac{z}{d} \right) \right] \qquad \text{[Eqn. 2-22]}$$

Estimation of the vertical profile shape factor was obtained by regressing both sides of Equation 2-22 for a number of cross-sections. Figure 2.14 is a graphical solution of Equation 2-22 where $1/sk$ is the slope; hence sk is the inverse of the slope.

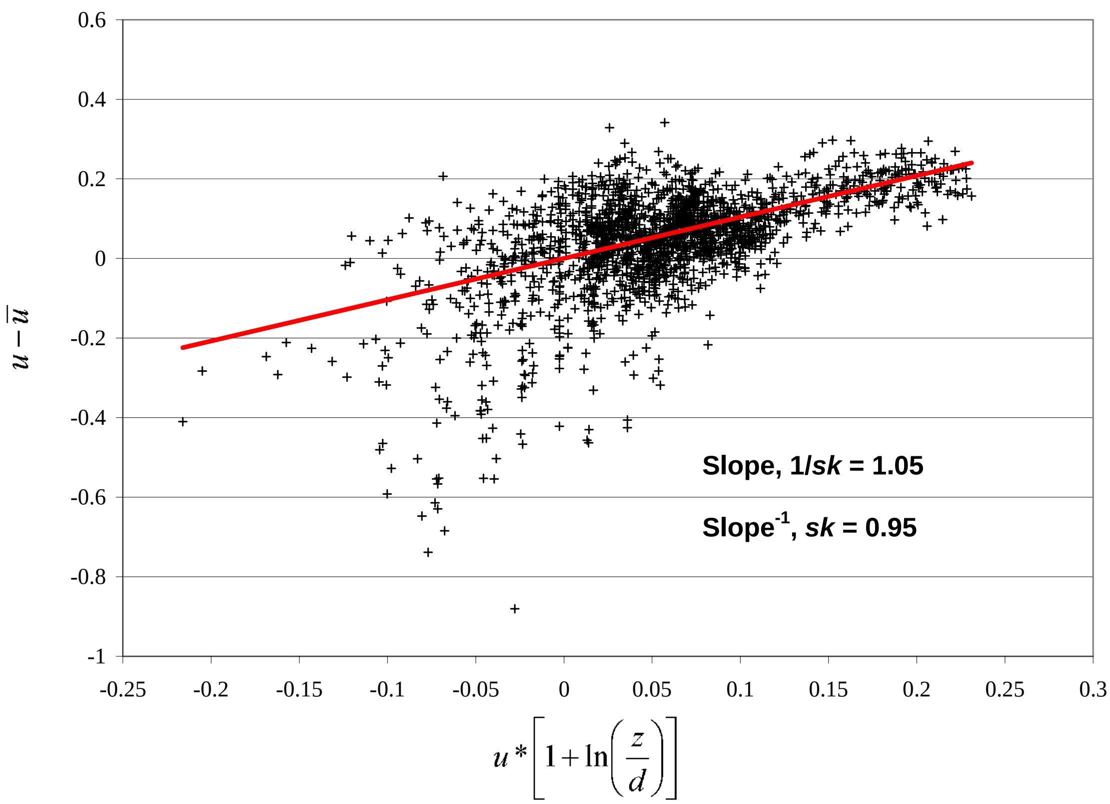

Figure 2.14: Regression of the Vertical Velocity Profile and Estimation of the von Karman Coefficient, *k*, and Shape Factor, *s*.

The regression of the graphical solution of Equation 2-22 was completed with 1928 data points and 90 individual profiles. The product of the shape factor (s) and von Karman (k) coefficient was found to be 0.95. Comparing a sample cross-section with the theoretical profile (Figure 2.15) shows a good representation. However, the 95 percent confidence interval illustrates the vast uncertainty in the point velocity across a give cross-section.

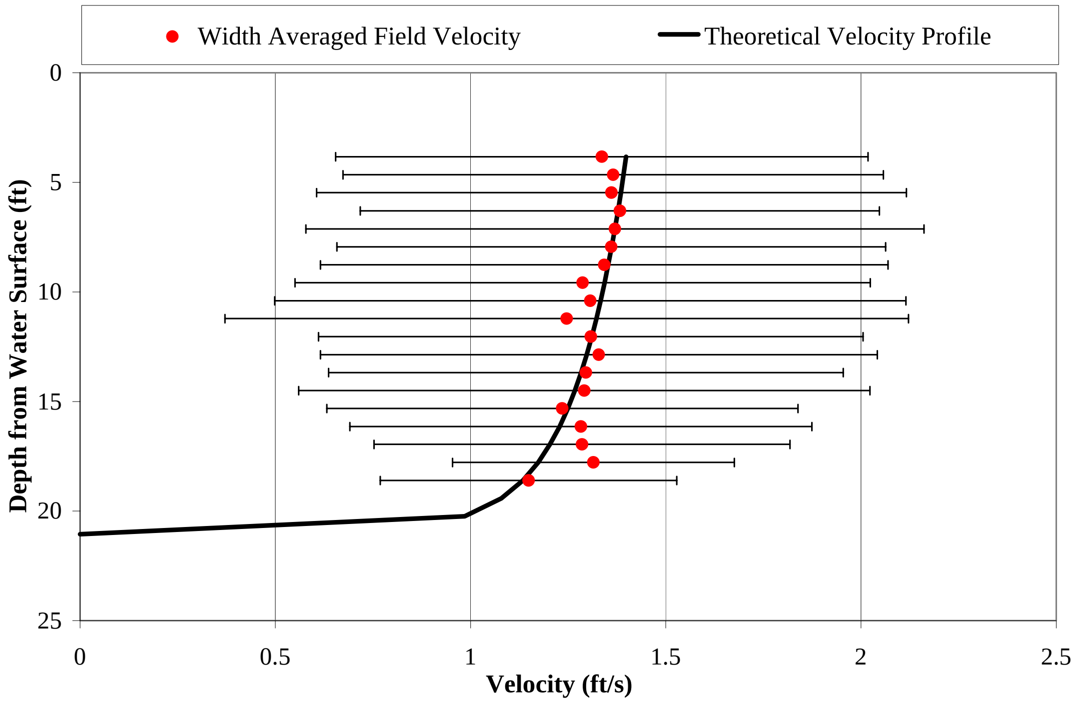

Figure 2.15: Theoretical Vertical Profile Compared to Field Velocity and 95% Confidence Intervals.

Estimating Transverse Profile Coefficients

Equations 2-2 and 2-5 were combined to estimate the transverse velocity coefficient. Assuming a depth averaged velocity ($F_V(z) = 1$), the longitudinal velocity across a channel can be described with Equation 2-23.

$$u(y) = \bar{u}\left[A + B\left(\frac{2y}{w}\right)^2 + C\left(\frac{2y}{w}\right)^4\right] \quad \text{[Eqn. 2-23]}$$

Substituting in Equations 2-8 and 2-9, the following relationship is obtained:

$$\frac{u}{\bar{u}} - 7.5\left[\left(\frac{2y}{w}\right)^2 - \left(\frac{2y}{w}\right)^4\right] = A\left[1 - 6\left(\frac{2y}{w}\right)^2 + 5\left(\frac{2y}{w}\right)^4\right] \quad \text{[Eqn. 2-24]}$$

For each cross-section, the depth averaged velocity is used in the estimation of a transverse velocity profile by regressing both sides of Equation 2-24. The point velocity (u) was the depth averaged velocity at each location across the cross-section. The average velocity ($\bar{u}$) was the average velocity of the average transverse velocity profile. The horizontal position (y) was the normalized distance across the channel with zero falling in the center of the channel. The width (w) was estimated using the starting point and ending point of the transect and the estimated distance to the bank.

The transverse velocity profile data used in Equation 2-24 provides an estimate for the transverse velocity profile shape coefficient, *A*. In Figure 2.16, the slope of the regression, which is the transverse shape coefficient *A*, was found to be about 1.34. The regression used 11894 data points from 149 profiles. Using Equation 2-8 the *B* coefficient was found to be -0.54 and using Equation 2-9 the *C* coefficient was found to be -0.8.

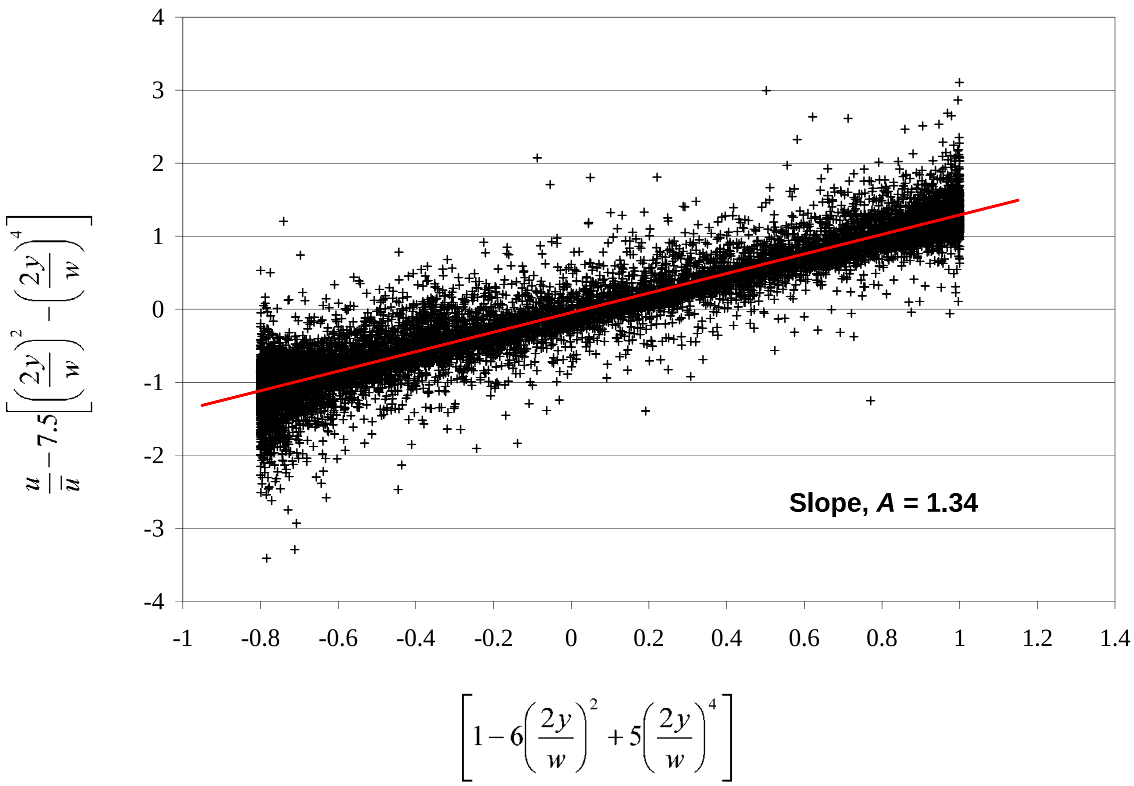

Figure 2.16: Regression of the Transverse Velocity Profile and Estimation of the Transverse Shape Coefficient, *A*.

A comparison of the theoretical profile and field profile (Figure 2.17) shows that the coefficients are a good representation of the velocity profile at this location. However, the 95 percent confidence interval illustrates the vast uncertainty in the point velocity across a give cross-section.

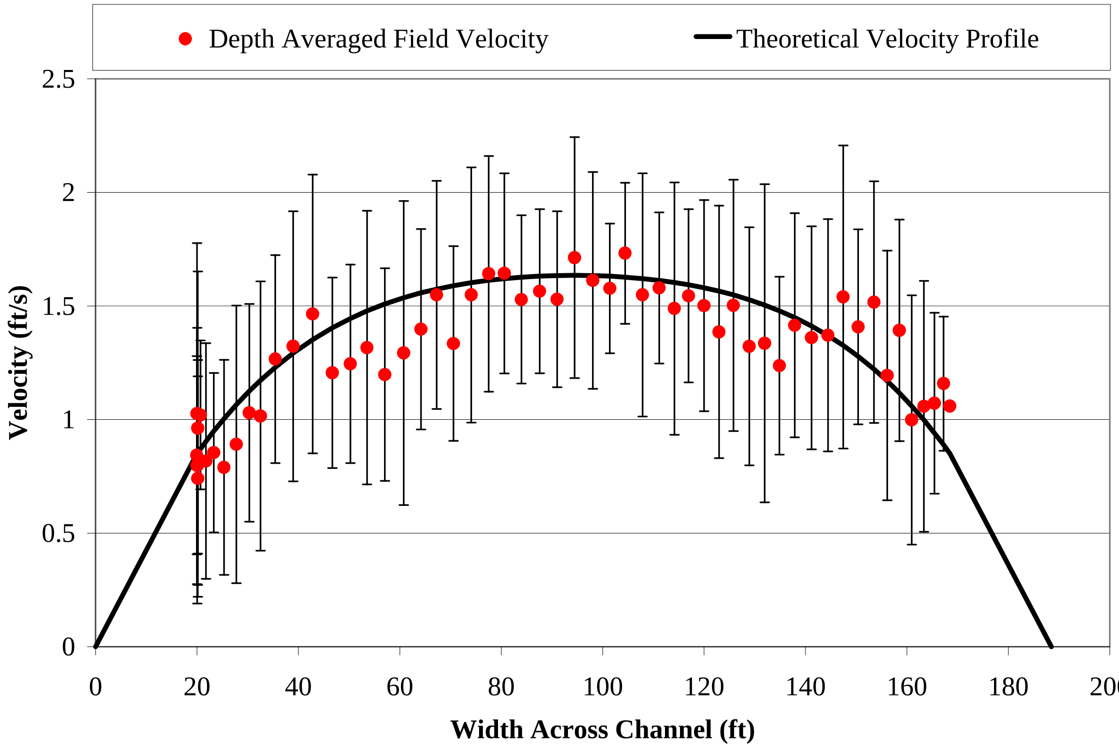

Figure 2.17: Theoretical Vertical Profile Compared to Field Velocity and 95% Confidence Intervals.

Calibration of Profile Shape Conclusions

The coefficients for the vertical and transverse profiles were found and are summarized in Table 2.1.

Table 2.1: Summary of Profile Coefficients Found from Field Data.

Coefficient	***Value***
Transverse *A*	1.34
Transverse *B*	-0.54
Transverse *C*	-0.80
Vertical *s*	2.38

2.5 Verification of PTM in a Single Channel – Static Stage

The longitudinal dispersion of the Particle Tracking Model was calculated using a simple channel with a steady flow. Dispersion coefficients for natural systems have been found to be quite varied and the theoretical range is enormous. This process is simply to show that the model is simulating dispersion within theoretical bounds.

2.5.1 Methods

Verification of dispersion used a theoretical 150,000 ft long channel with a width of 500 ft and a 0% bottom slope. Stage at the downstream boundary was set at 40 ft. The upstream boundary was forced with three separate positive flows, 10,000, 32,000, and 64,000 cfs, giving an average velocity in the channel of 0.5, 1.6, and 3.2 ft/s respectively.

Parameters assumed for the model were: transverse flow coefficient, C_T, of 0.6; shear velocity, u/u*, of 0.1; vertical profile shape coefficient, *s*, of 2.375 (Table 2.1); and transverse *A*, *B* and *C* shape coefficients of 1.34, -0.54, and -0.8 (Table 2.1).

The model was compared to the theoretical values using Equation 2-1. Because it is difficult to determine the actual parameters that represent the Sacramento – San Joaquin Delta, theoretical parameters, which bracket the higher and lower bounds of dispersion, are shown in Table 2.2.

Table 2.2: Range of Parameters Used to Estimate the Dispersion Coefficient.

Parameter	Value(s)	Reference
C_T	0.6	Fischer (1979)
u/u*	0.1	Fischer (1979)
h	1.0W to 0.5W	Fischer (1979)
$\overline{u}'^2$	$0.03\overline{u}^2$ to $0.2\overline{u}^2$	Fischer (1979)
I	0.01 to 0.03	Bogle (1997)

Applying these assumptions results in two equations that bound the theoretical range of dispersion. Using I = 0.01, h = 0.5 W, and $\overline{u}'^2 = 0.03\overline{u}^2$ for the lower bound, the following equation can then be deduced:

$$K = \frac{0.00125\overline{u}W^2}{d} \qquad \text{[Eqn. 2-25]}$$

Using I = 0.03, h = 1.0 W, and $\overline{u}'^2 = 0.2\overline{u}^2$ for the upper bound, the following equation can then be deduced:

$$K = \frac{0.1\overline{u}W^2}{d} \qquad \text{[Eqn. 2-26]}$$

Results from the calculation of the upper and lower bounds of the dispersion coefficient for each of the flow scenarios is shown in Table 2.3.

Table 2.3: Theoretical Bounds on the Dispersion Coefficient.

Flow (cfs)	Velocity (ft/s)	Lower Bound (ft^2/s)	Upper Bound (ft^2/s)
64,000	3.2	25	2000
32,000	1.6	13	1000
10,000	0.5	4	312

For each of the three simulations particles were randomly inserted at the upstream end of the long channel. The longitudinal distance along the channel for each particle was collected every five minutes. The variance of the particle plume was calculated for each time step. The respective dispersion for each time step was then determined by half the slope (half of the derivative of the variance) (Figure 2.1).

2.5.2 Results

The results of the dispersion verification resulted in consistent results for the three flow scenarios with respect to the upper and lower bounds.

The 64,000 cfs flow scenario resulted in an average velocity of 3.2 ft/s. The simulation ended after 700 minutes (Figure 2.18) when the first particle reached the end of the theoretical channel. Theoretical longitudinal dispersion for this channel and velocity ranged from 25 to 2000 ft^2/s. The particles became fully dispersed within 60 minutes of simulation. However, after the first 60 minutes, the dispersion coefficient continued to rise from around 600 to 900 ft^2/s.

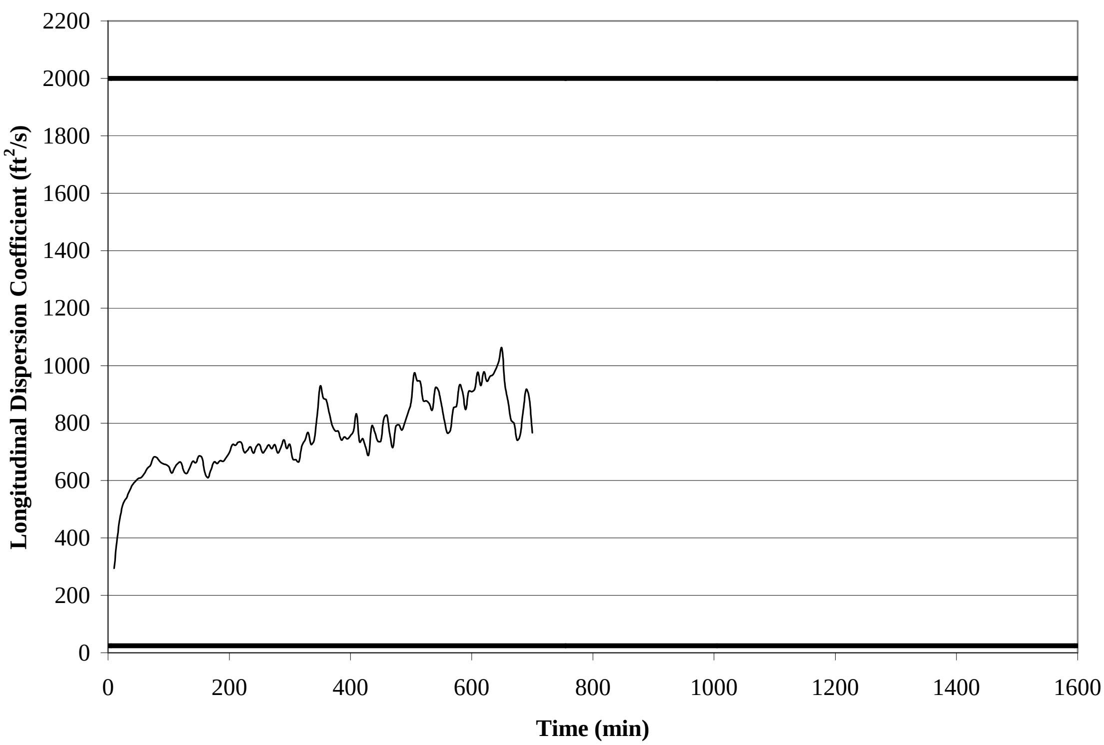

Figure 2.18: Theoretical Estimate of PTM Longitudinal Dispersion Coefficient for an Average Velocity of 3.2 ft/s.

The 32,000 cfs flow scenario resulted in an average velocity of 1.6 ft/s. The simulation ended after 1330 minutes (Figure 2.19) when the first particle reached the end of the channel. Theoretical longitudinal dispersion ranged from 13 to 1,000 ft^2/s. The particles became fully dispersed within 80 minutes of simulation. The dispersion coefficient at a velocity of 1.6 ft/s for PTM is approximately 400 ft^2/s.

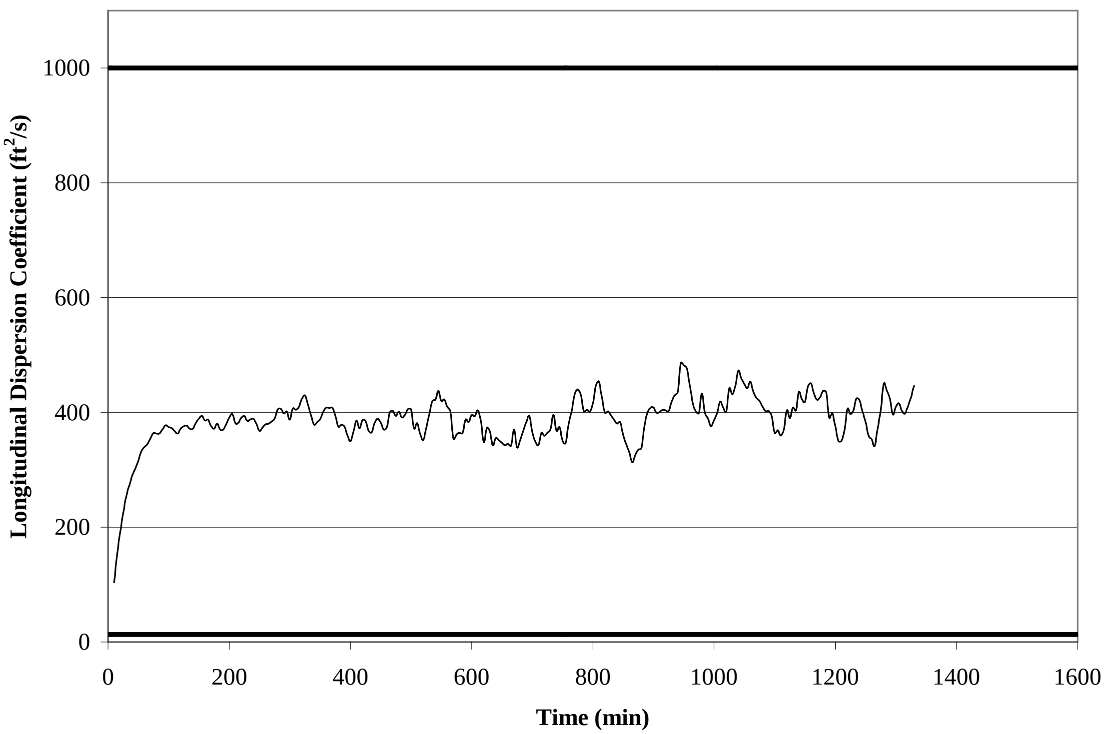

Figure 2.19: Theoretical Estimate of PTM Longitudinal Dispersion Coefficient for an Average Velocity of 1.6 ft/s.

The 10,000 cfs flow scenario resulted in an average velocity of 0.5 ft/s. The simulation was run for 1440 minutes (Figure 2.20). At that point all particles remained within the channel. Theoretical longitudinal dispersion ranged from 4 to 312 ft^2/s. Full dispersion occurred within 200 minutes of the simulation. At a velocity of 0.5 ft/s for PTM, the dispersion coefficient was approximately 125 ft^2/s.

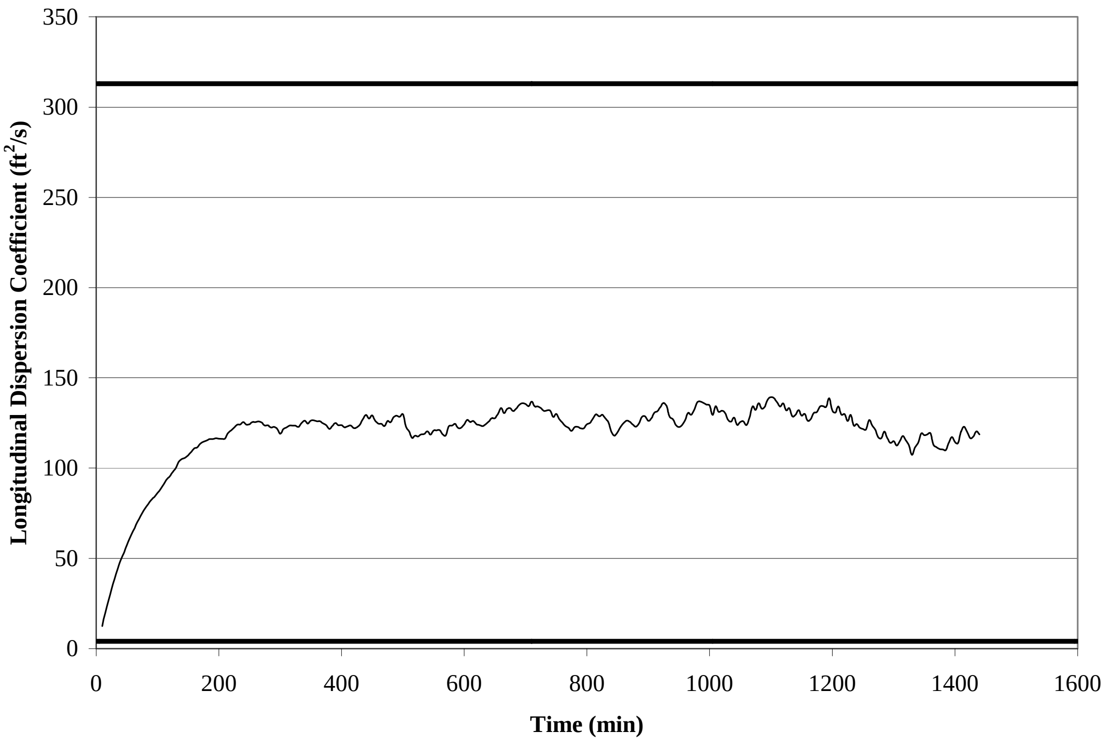

Figure 2.20: Theoretical Estimate of PTM Longitudinal Dispersion Coefficient for an Average Velocity of 0.5 ft/s.

2.5.3 Verification Discussion

The process of verifying the dispersion of PTM has produced successful results. PTM has proven to simulate dispersion in a consistent manner. For the three different velocity scenarios, the dispersion coefficient was consistently found to be between the lower and upper bounds.

2.6 Future Directions

The validation of the model is being completed. There are a number of physical studies for which PTM may simulate in the validation process. These studies include the:

- 1997 Dye Study.

  In the spring of 1997 the USGS (Oltmann, 1998) conducted a dye study where rhodamine WT dye was inserted into the San Joaquin river near Mossdale bridge. The dye concentration was monitored at various locations in the Delta.

- 1993 striped bass egg data.

  In late 1993 during the striped bass spawn, egg densities were collected along the

Sacramento River. Striped bass lay their eggs at the surface of the water column. The eggs then slowly sink as they move downstream due to being slightly more dense than the water.

- 2000 Delta Cross Channel study.

  In fall 2000 the USGS, DWR, U.S. Fish and Wildlife Service (USFWS), and others participated in a study of the flow around the Delta Cross Channel. From this study resulted in an extensive data set that shows the movement of water around the cross channel for many different flow conditions.

2.7 References

Bogle, G. (1997). "Stream Velocity Profiles and Longitudinal Dispersion." *Journal of Hydrologic Engineering.* American Society of Civil Engineers. 123 (9).

Bogle, G. (1994). "Simulation of Dispersion in Streams by Particle Tracking." *Draft Report*. Water Engineering & Modeling.

Denton, R. (1995). "Particle Tracking with Non-Uniform Cross-Sectional Mixing." Presentation given at the Bay-Delta Modeling Forum. Monterey, CA.

Dimou, K. Nadia and Adams, E. Eric (1993). "A Random-walk, Particle Tracking Model for Well Mixed Estuaries and Coastal Waters." *Estuarine, Coastal and Shelf Science.*

Fischer, H.B., E.J. List, R.C.Y. Koh, J. Imberger, N.H. Brooks. (1979). Mixing in Inland and Coastal Waters. Academic, New York.

Miller, Aaron. (2000). "Chapter 5: DSM2 Particle Tracking Model Development." *Methodology for Flow and Salinity Estimates in the Sacramento-San Joaquin Delta and Suisun Marsh. 21st Annual Progress Report to the State Water Resources Control Board.* California Department of Water Resources. Sacramento, CA.

Nader-Tehrani, P. (2001). "Chapter 2: DSM2 Calibration and Validation." *Methodology for Flow and Salinity Estimates in the Sacramento-San Joaquin Delta and Suisun Marsh. 22nd Annual Progress Report to the State Water Resources Control Board.* California Department of Water Resources. Sacramento, CA.

Oltmann, R. N. (1998). *Measured Flow and Tracer – Dye Data Showing Anthropogenic Effects on the Hydrodynamics of South Sacramento – San Joaquin Delta, California, Spring 1996 and 1997.* United States Geological Survey, Open File Report 98-285.

RD Instruments. (1995). ADCP River Discharge Measurement Manual.

Smith, T. (1993). "Chapter 2: Particle Tracking Model for the Delta." *Methodology for Flow and Salinity Estimates in the Sacramento-San Joaquin Delta and Suisun Marsh. 14th Annual Progress Report to the State Water Resources Control Board.* California Department of Water Resources. Sacramento, CA.

Smith, T. (1998). "Chapter 4: DSM2 PTM." *Methodology for Flow and Salinity Estimates in the Sacramento-San Joaquin Delta and Suisun Marsh. 19th Annual Progress Report to the State Water Resources Control Board.* California Department of Water Resources. Sacramento, CA.

Wilbur, R. (2000). *Validation of Dispersion Using the Particle Tracking Model in the Sacramento-San Joaquin Delta*. M.S. Thesis. University of California, Davis.